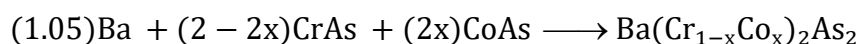


## Supplementary Material to the article “NMR spectroscopy of solid solutions of new layered arsenides Ba(Cr<sub>1-x</sub>Co<sub>x</sub>)<sub>2</sub>As<sub>2</sub>”

### Experimental methods.

#### Synthesis of Ba(Cr<sub>1-x</sub>Co<sub>x</sub>)<sub>2</sub>As<sub>2</sub> {x = 0.0, 0.2, 0.3, 0.6, 0.8, 1.0}

All operations for the synthesis of Ba(Cr<sub>1-x</sub>Co<sub>x</sub>)<sub>2</sub>As<sub>2</sub> {x = 0.0, 0.2, 0.3, 0.6, 0.8, 1.0} and precursors CrAs, CoAs, except for heat treatment, were performed in a dry argon glove box with oxygen and water vapor content less than 0.1 ppm. To obtain polycrystalline samples of Ba(Cr<sub>1-x</sub>Co<sub>x</sub>)<sub>2</sub>As<sub>2</sub> {x = 0.0, 0.2, 0.3, 0.6, 0.8, 1.0} barium metal chips (99.8%, LANHIT) were mixed with previously obtained cobalt and chromium monoarsenides according to the scheme shown below:



An excess of 5% barium compensates for losses caused by its volatility. The aluminum crucible with the reaction mixture was placed in a quartz ampoule, which was evacuated to a residual pressure of  $5 \cdot 10^{-6}$  bar and sealed, after it was annealed in a furnace at of 850 °C (heating rate was 50 °C/h) for 10 hours. The sintered product obtained after annealing was homogenized by grinding and pressed. The resulting tablets were also placed in a aluminum crucible, sealed in a quartz ampoule, and annealed in the oven at of 900 °C (heating rate was 100 °C/h) for 25 hours. If necessary (based on the results of X-ray phase analysis of the samples obtained after the second annealing), the samples were repeatedly homogenized and annealed in a manner identical to the second stage.

#### Characterisation

For phase composition and crystal structure analysis of Ba(Cr<sub>1-x</sub>Co<sub>x</sub>)<sub>2</sub>As<sub>2</sub> polycrystalline samples, the X-ray diffraction analysis was carried out with a Huber Guiner G670 diffractometer (Cu K<sub>α1</sub> radiation). The X-ray diffraction patterns were analyzed using the Jana2006 software and the Rietveld method for the samples crystal structure and quantitative composition refining (fig. S1) [1].

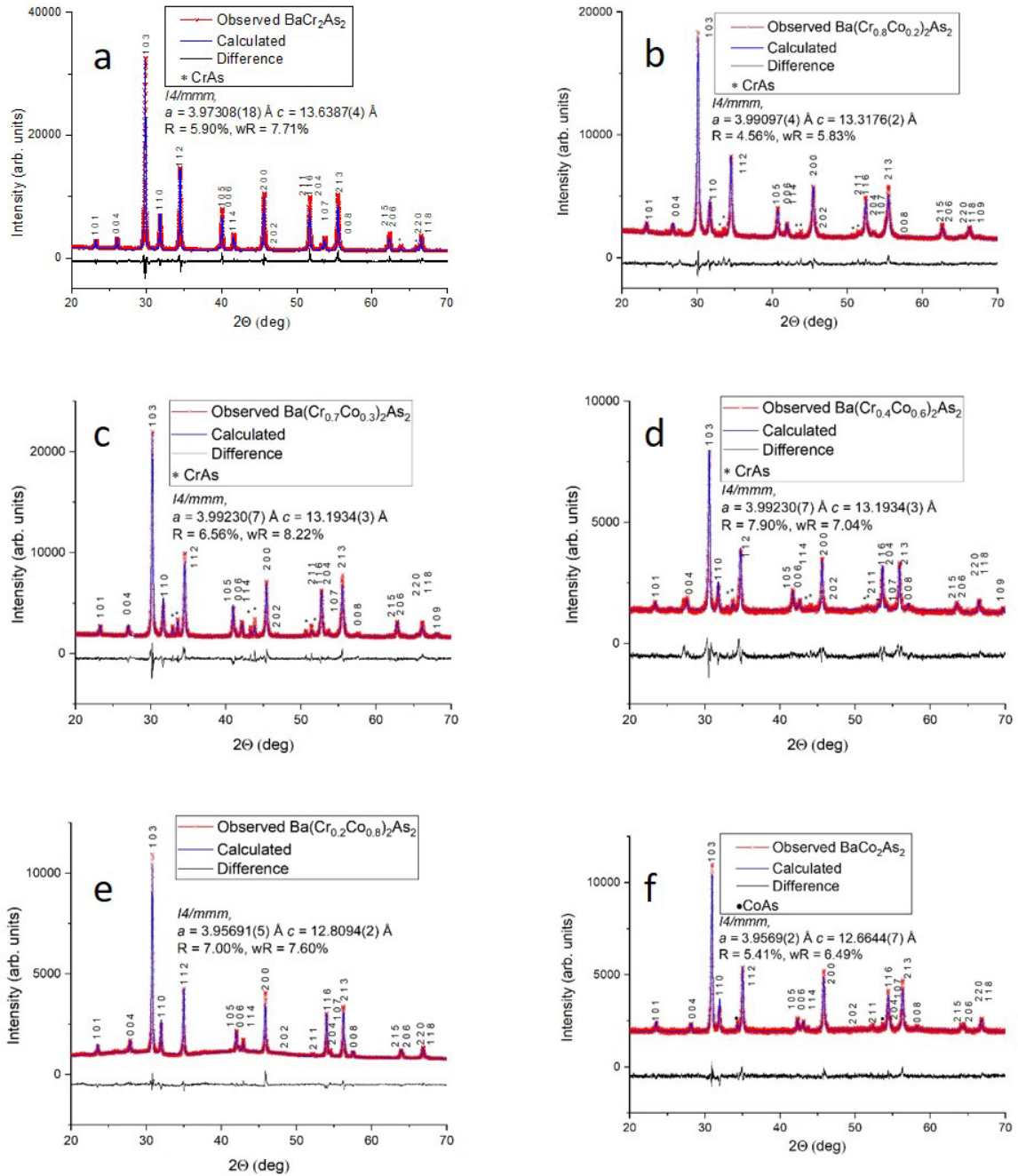


Fig. S1. Observed, calculated and difference X-ray diffraction patterns for solid solutions samples  $\text{Ba}(\text{Cr}_{1-x}\text{Co}_x)_2\text{As}_2$   $\{x = 0.0, 0.2, 0.3, 0.6, 0.8 \text{ and } 1.0; \text{ a - f, respectively}\}$ . For each composition the unit cell parameters obtained as a result of the Rietveld method refinement are given, as well as a Bragg and weight uncertainty factors,  $R$  and  $wR$ , respectively [2, 3].

### NMR spectroscopy

NMR spectra were measured on  $^{59}\text{Co}$  nuclei (nuclear spin  $I = 7/2$ , gyromagnetic ratio  $^{59}\gamma/2\pi = 10.08 \text{ MHz/T}$ , quadrupole moment  $eQ = 0.41 \text{ barn}$ , natural abundance 100%) and  $^{75}\text{As}$  nuclei (nuclear spin  $I = 3/2$ , gyromagnetic ratio  $^{75}\gamma/2\pi = 7.32 \text{ MHz/T}$ , quadrupole moment  $eQ = 0.31 \text{ barn}$ , natural abundance 100%) [4] at temperatures of 4.2 K (for all samples) and additionally at 150 K for the  $\text{Ba}(\text{Cr}_{0.4}\text{Co}_{0.6})_2\text{As}_2$  sample. NMR spectra were recorded using the

standard Hahn spin echo method with a  $\pi/2$  and  $\pi$  radio frequency (RF) pulse sequence on a fully digital phase-coherent pulse spectrometer. RF pulses were generated by a direct digital synthesis (DDS) board, and digital quadrature detection was performed directly on the carrier frequency. The spectra were recorded as the integral of the spin echo magnitude in the time domain with a step sweep of the magnetic field (NMR at a fixed frequency of 40.0 MHz) or frequency (NMR in zero external magnetic field). Optimization of the pulse sequence parameters: duration and power of pulses, delay between them, repetition time of the pulse sequence and number of accumulations was performed separately for each type of nuclei.

#### Analysis and simulation of the NMR spectrum of $^{75}\text{As}$ nuclei in $\text{BaCo}_2\text{As}_2$

The  $^{75}\text{As}$  NMR spectrum of  $\text{BaCo}_2\text{As}_2$  has a pronounced asymmetric shape with a noticeable shoulder on the left side and can be qualitatively represented as a sum of two spectra, as shown in Fig. S2. The spectrum from the main phase of  $\text{BaCo}_2\text{As}_2$  is a polycrystalline NMR spectrum with a quadrupole frequency  $\nu_Q = 1.18$  MHz, an asymmetry parameter  $\eta = 0.26$  and an isotropic shift  $K_{\text{iso}} = +1.3\%$  (gray spectrum in Fig. S2).

The above estimate of the isotropic Knight shift  $K_{\text{iso}} = +1.3\%$  is in excellent agreement with the results [5] obtained for the  $\text{BaCo}_2\text{As}_2$  single crystal at 4.2 K:  $K_{\text{iso}} = +1.38\%$ . This is the highest value in the entire  $\text{Ba}(\text{Cr}_{1-x}\text{Co}_x)_2\text{As}_2$  series, which indicates the maximum value of the density of states at the Fermi level  $N(E_F)$  for a sample with a cobalt content of 100% and is in good agreement with the low residual resistance  $\rho_{0,ab} = 5.1 \mu\Omega\cdot\text{cm}$  observed in the  $(a,b)$  plane in the  $\text{BaCo}_2\text{As}_2$  single crystal [5]. The obtained value of  $\nu_Q$  is in good agreement with the literature data on  $\text{BaCo}_2\text{As}_2$ : 0.96 MHz at 4.2 K [6] and 0.8 MHz at 1.6 K [5].

As for the additional singlet (without visible quadrupole splitting) line (blue spectrum in Fig. S2), this is probably the central transition of the impurity phase  $\text{CoAs}$ , the content of which in the  $\text{BaCo}_2\text{As}_2$  sample, according to X-ray phase analysis, is  $\approx 6\%$ . It is also possible that this impurity is partially amorphous, which may lead to an underestimation of its content by X-ray diffraction methods, although it is clearly visible in the NMR spectrum. It should be noted that in the papers [5, 6] single-crystal samples of  $\text{BaCo}_2\text{As}_2$  were studied, and no additional lines were observed in the  $^{75}\text{As}$  spectra there.

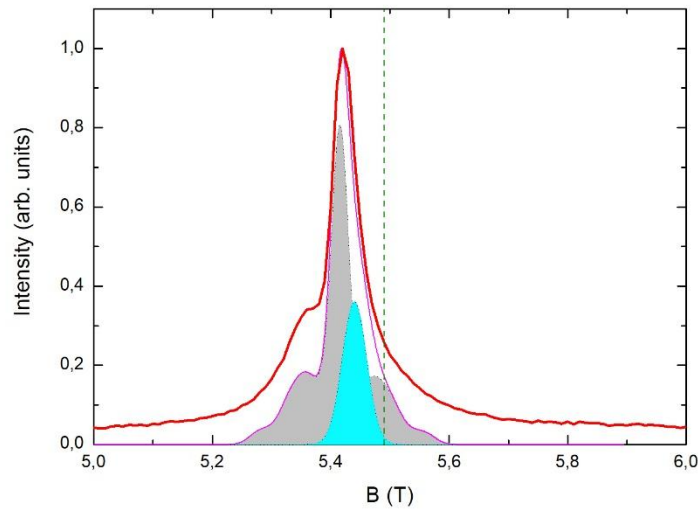


Fig. S2. NMR spectrum of  $^{75}\text{As}$  nuclei in  $\text{BaCo}_2\text{As}_2$  measured at a fixed frequency of 40 MHz at  $T = 4.2$  K. The vertical dashed line indicates the position of the Larmor field  $^{75}B_L = 5.46$  T for  $^{75}\text{As}$  nuclei at a frequency of 40 MHz. The gray and blue filled spectra are theoretical simulations describing the signal from the main and impurity phases, respectively, performed using the Simul program [7], the solid purple line is the total theoretical spectrum.

Comparison of NMR spectra of  $^{75}\text{As}$  and  $^{59}\text{Co}$  nuclei in the compound  $\text{Ba}(\text{Cr}_{0.4}\text{Co}_{0.6})_2\text{As}_2$  in the paramagnetic and magnetically ordered state

The sample of the composition  $\text{Ba}(\text{Cr}_{0.4}\text{Co}_{0.6})_2\text{As}_2$ , according to preliminary measurements of magnetic susceptibility and *ab-initio* calculations [8], has a magnetic transition temperature  $T_N \approx 111$  K in the temperature range accessible to our NMR spectrometer, in contrast to compositions with  $x = 0, 0.2$  and  $0.3$ , where  $T_N$  is significantly higher than the room temperature. This provides a unique opportunity to compare NMR spectra above and below the transition for both  $^{75}\text{As}$  (Fig. S3, right panel) and  $^{59}\text{Co}$  nuclei (Fig. S3, left panel).

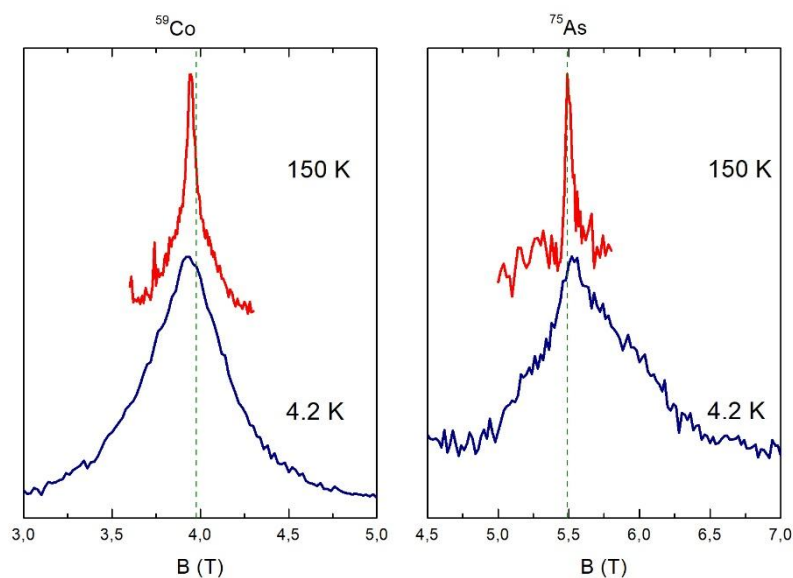


Fig. S3. NMR spectra at  $T > T_N$  (upper spectra) and  $T < T_N$  (lower spectra) for  $^{75}\text{As}$  (right panel) and  $^{59}\text{Co}$  (left panel) nuclei for the compound  $\text{Ba}(\text{Cr}_{0.4}\text{Co}_{0.6})_2\text{As}_2$ . Dashed lines are the positions of the Larmor fields ( $^{59}\text{B}_L = 3.97$  T for  $^{59}\text{Co}$  nuclei and  $^{75}\text{B}_L = 5.46$  T for  $^{75}\text{As}$  nuclei).

From Fig. S3 it can be seen that the NMR spectra of both types of nuclei exhibit similar behavior during the transition from the paramagnetic ( $T = 150$  K) to the magnetically ordered ( $T = 4.2$  K) state. Quite narrow lines at high temperature:  $^{75}\text{FWHM}_{60}(150\text{K}) = 0.084$  T and  $^{59}\text{FWHM}_{60}(150\text{K}) = 0.094$  T broaden noticeably at 4.2 K to 1.0 and 0.54 T for  $^{75}\text{As}$  and  $^{59}\text{Co}$  nuclei, respectively. This indicates the occurrence of induced local magnetic fields on the  $^{75}\text{As}$  and  $^{59}\text{Co}$  nuclei with a significant spread in their values in the  $\text{Ba}(\text{Cr}_{0.4}\text{Co}_{0.6})_2\text{As}_2$  compound. At the same time, the magnitude of the isotropic shift of both nuclei remains practically unchanged, which indicates the invariance of the electronic structure of the  $\text{Ba}(\text{Cr}_{0.4}\text{Co}_{0.6})_2\text{As}_2$  compound during the transition from the paramagnetic to the magnetically ordered state.

1. V. Petříček, M. Dušek, L. Palatinus, *Zeitschrift für Kristallographie - Crystalline Materials* 5, 345 (2014). <https://doi.org/10.1515/zkri-2014-1737>
2. W.I.F. David *Powder Diffraction: Least-Squares and Beyond*. *J Res Natl Inst Stand Technol.* 2004 Feb 1;109(1):107-123. <https://doi.org/10.6028/jres.109.008>
3. Vitalij K. Pecharsky, Peter Y. Zavalij, *Fundamentals of Powder Diffraction and Structural Characterization of Materials*, Second Edition, Springer New York, XXIV, 744, <https://doi.org/10.1007/978-0-387-09579-0>
4. NMR Periodic Table // URL: <https://periodic.pastis.dk>

5. V. K. Anand, D. G. Quirinale, Y. Lee, B. N. Harmon, Y. Furukawa, V. V. Ogloblichev, A. Huq, D. L. Abernathy, P. W. Stephens, R. J. McQueeney, A. Kreyssig, A. I. Goldman, D. C. Johnston, Phys. Rev. B 90, 06451, 2014, <https://doi.org/10.1103/PhysRevB.90.064517>
6. K. Ahilan, T. Imai, A. S. Sefat, F. L. Ning, Phys. Rev. B 90, 014520, 2014, <https://doi.org/10.1103/PhysRevB.90.014520>
7. Gerashchenko A.P., Volkova Z.N., Sadykov A.F., Smol'nikov A.G., Piskunov Y.V., Mikhalev K.N., ZhETF - 2025. - Vol. 167. - N. 4. - P. 553–570.  
<https://doi.org/10.31857/S0044451025040091>
8. Gippius, A.A., Mironov, A.V., Shilov, A.I. et al. Synthesis, Crystal Structure, and Structural Features of Solid Solutions  $\text{Ba}(\text{Cr}_{1-x}\text{Co}_x)_2\text{As}_2$  - New Layered Arsenides with the  $\text{ThCr}_2\text{Si}_2$  Structure. J Struct Chem 66, 1306–1316 (2025). <https://doi.org/10.1134/S0022476625060150>